REFINING SOUTH POLE-AITKEN BASIN RING STRUCTURE USING GRAVIMETRY AT MASSIFS

J. M. Walsh, A. M. Bailey, R.V. Wagner, M. R. Henriksen, H. Bernhardt, A. K. Boyd, M. S. Robinson, School of Earth and Space Exploration, Arizona State University, Tempe, AZ (jessica.walsh.1@asu.edu)

Introduction: The South Pole-Aitken (SPA) basin is thought to be the largest and oldest impact basin on the lunar surface [**1**]. It underlies every impact basin near the south pole and extends north to Aitken Crater (16°S, 173°E). Due to its ancient age of 4.26 ± 0.03 Ga [**2**], the rings of this ~2600 km basin are significantly degraded, and in the western half they are almost entirely absent, making mapping the ring structures a challenge. Accurately reconstructing the SPA ring structures is key to understanding the basin's formation.

Previous work identified three possible ring structures for the SPA basin [**3**] (**Fig**. 1); however, the western portions remain ambiguous with no significant elevation drops to identify basin rings. Two other studies attempted reconstruction of the western area [**4**, **5**] with best-fit ellipses to the partial ring identifications.

Here, we manually reconstruct the full extent of the SPA ring structures from local massif formations [**4**], crustal thickness, Bouguer gravity, and previously established partial rings [**3**]. The partial outermost ring structure from [**3**] (**Fig. 1**) is in agreement with the one partial ring structure identified in [**6**] (**Fig.1**).

Data & Methods: We identified and characterized massif extents by measuring "total relief" (relief from the base elevation to the summit elevation) and "prominence relief" (relief of the mountain peak relative to the lowest encompassing 100 m contour interval that contains no other peak) [**4**] from the Lunar Reconnaissance Orbiter Camera (LROC) Wide Angle Camera (WAC) GLD100 topographic map [**7**]. These measurements provide heights that can be compared globally and locally

A mountain is defined as an "elevated landform that rises prominently above its surroundings" [**8**]. Since the terrestrial definition includes sea level [**8**], we measured landforms that rose 457.2 m or more above neighboring landforms to match the 1500 ft elevation established by [**8**]. Here we analyzed mountains with total relief greater than 6000 meters.

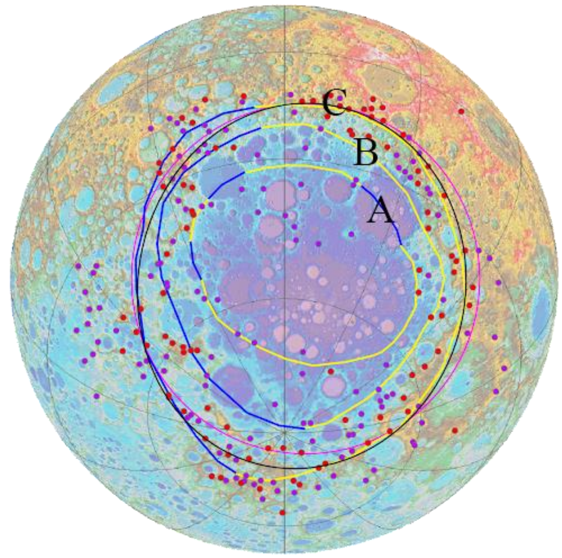

***Figure 1**. SPA basin with ring structures overlain on GLD100 (orthographic projection centered at 56° S,180°E) [**7**]. Massifs >6000m (red) and <6000m total relief (purple), best-fit mountain ellipse (black), Hiesinger [**3**] rings (yellow), Spudis [**6**] ring (pink), and our rings (blue).*

The map of these mountains is then compared visually to crustal thickness and Bouguer gravity (degree and order 660) maps of the region [**9**]. Even if any clear massif chains of high total relief (>6000 m) (**Fig. 1** in red) were absent, we continued the rings along an annular, positive Bouguer anomaly or the highest crustal thickness gradient.

Additionally, we created a "best-fit" ellipse of all the mountains measured in SPA using an equation from [**10**] as a quantitative way to estimate the extent of the basin. This best-fit ellipse measures 3040 km x 2268 km in orthographic projection. The ellipse and the rings mapped by hand align well with the outermost ring of SPA, as drawn by [**3,6**] (Fig.1, yellow and pink)

We mapped the geographic extent of each mountain in QGIS [**11**] and then sorted the mountains into four categories associated with the median from the Bouguer Gravity disturbance map [**9**]: low (-25 mGal and lower), neutral (-25 to 25 mGal), high (25 mGal and higher), and ambiguous (containing both extremely low (>-120 mGal) and extremely high (>120 mGal) anomalies within its perimeter).

Results & Discussion: On average, mapped mountains rise in total relief from the innermost ring A (~5-6 km) to the outermost ring C (~6-7 km) (**Fig. 1**). The average crustal thickness and regional elevation also increase moving out from the basin interior, and other large basins (such as Orientale) increase in mountain elevation from interior to exterior based on profiles drawn using [**12**]. However, on average, prominence relief does not change significantly between rings (~1-2 km).

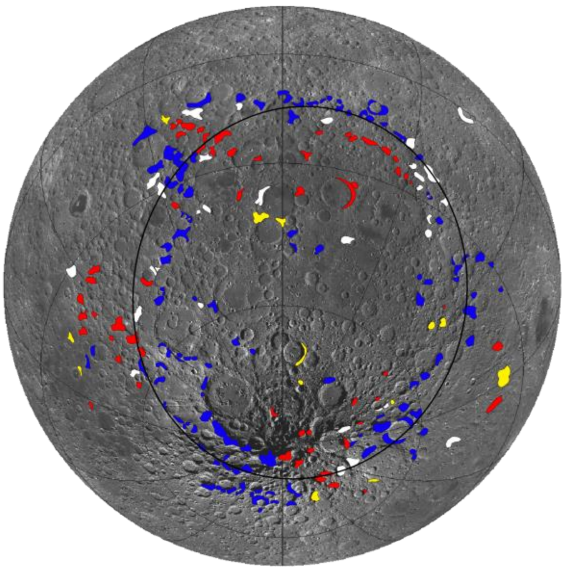

Figure 2. *SPA basin WAC Global image mosaic orthographic projection, centered at 56° S, 180° E [**12**]. Massifs with low Bouguer gravity (blue), neutral (yellow), high (red), and ambiguous Bouguer gravity (white), with our best-fit ellipse (3040 km x 2268 km)(black).*

We observed some spatial patterns correlating the mountains with Bouguer gravity anomalies within SPA (**Fig. 2**). Most mountains in SPA have negative Bouguer gravities, indicating isostatic equilibrium, with a lower density crust underneath the mountains [**13**].

Negative Bouguer mountains appear to wrap around SPA in a ring-like structure consistent with partial rings from [**3,6**] and our best fit ellipse. One interpretation of this is that the outermost mapped ring C (**Fig. 1**) of SPA is the result of the collapse of the basin transient cavity, similar to the Outer Rook Ring of Orientale [**5**]. Brecciated crust and Mountains with thickened crust which are at least partially equilibrated form a majority of the structures between the two outer rings (B, C). With this interpretation, the middle ring, B (Fig.1), would be a close approximation for the transient crater rim, similar to the Inner Rook Ring of Orientale [**5**] and consistent with conclusions drawn by [**3,5**].

An alternate interpretation ring C is that this is the location of the transient crater cavity rim similar to the "Inner Rook Ring" at Orientale basin, implying that the furthest mountains mapped here are part of the larger collapsed ring ~3600 km in diameter that passes through the edge of Orientale basin.

SPA could be more elliptical than previously suggested, as one could fit the low Bouguer gravity mountains with a more elongated ellipse than our best-fit ellipse (Fig. 2) and ellipses fit in previous work [**5**].

Based on analysis from this research, there is no evidence from massifs of the interior ring [**3**] that was based on Clementine topographic data.

Conclusion: Our investigation into the reconstruction of SPA's significantly degraded rings and analysis of Bouguer gravity underneath is consistent with [**3**] for the location of ring C and the possibility that it might be related to the collapse of SPA's transient crater. Ring B (Fig. 1) was also in agreement in location with [3]. However, it cannot be ruled out that the transient crater cavity could have been as large as ring C.

The correlation drawn from mountains with low Bouguer gravity within basin rings deserves further investigation, as does the possibility of a 4th basin ring with a diameter of ~3600 km. A comparison between the massifs of giant impacts on the Moon could help to further our understanding of basin formation and degradation on all planetary surfaces.

References: [**1**] Wilhelms, D.E. (1987), GHM, USGS, [**2**] Hiesinger, H. et al. (2012), *LSC XLIII*, abstract #2863, [**3**] Hiesinger and Head (2003) *Microsymp. 38*, MS101, [**4**] Bailey et al. (2020) *LSC LIII*,#1753, [**5**] J.W. Head et al. (1993) JGR, 170-176 [**6**] Spudis, P. D. (1993), *The Geology of Multi-ring Basins* [**7**] Scholten, F., (2012). *JGR-P*, 117(E12). [**8**] Fry et al. (1987) SUMMIT, pp 16-32, [**9**] Andrews-Hanna, J. C. et al. (2014), *Nature,* 514, 68-71. [**10**] G. Taubin (1991) *IEEE Trans. PAMI*, 13, pages 1115-1138, [**11**] ESRI (2021) ArcGIS v.10.6.1, [**12**] Robinson et al. (2010) *SSR* 150, 55 [**13**] M. Eshagh (2021) *Satellite Gravimetry and the Solid Earth*, pp 263-312.